Large-Area Oxidation of AlAs Layers for Dielectric Stacks and Thick Buried Oxides

S.N. TANDON,[1,3] J.T. GOPINATH,[1] A.A. ERCHAK,[1,2] G.S. PETRICH,[1] L.A. KOLODZIEJSKI,[1] and E.P. IPPEN[1]

1.—Research Laboratory of Electronics, Massachusetts Institute of Technology, Cambridge, MA 02139. 2.— Currently with Luminus Devices, Inc., Woburn, MA 01801. 3.—E-mail: tandon@mit.edu

The wet oxidation of AlAs and AlGaAs has been limited to relatively small lateral dimensions and relatively thin layers. Approaches are described to extend the oxide dimensions both horizontally and vertically, creating large-area and thick buried oxides. Two types of large-area structures are examined: dielectric stacks with thin buried oxides and semiconductor-on-insulator structures with thick buried oxides. Low Al-content AlGaAs layers with low oxidation rates are used as the high-index layers in large-area dielectric-stack structures. High Al-content AlGaAs layers with low volume contraction are used to create stable, thick buried oxides with millimeter-scale areas.

Key words: AlGaAs oxidation, lateral oxidation, dielectric stacks, buried oxides

INTRODUCTION

The ability to transform AlAs and (Al,Ga)As with high aluminum content into aluminum oxide using a wet thermal-oxidation process has had many important and beneficial consequences. Previous work focused on the use of oxidized Al-containing materials as the index-guiding layer in edge-emitting lasers,[1] as current confinement layers in vertical-cavity surface-emitting lasers,[2–5] as low dielectric-constant layers in distributed Bragg mirror stacks,[6–9] and as low index of refraction materials suitable for optical confinement when integrated with high-index materials.[10,11] Electronic use of oxidized Al-containing material was investigated as a gate dielectric for GaAs-based transistor[12–14] structures similar to the well-studied Si/SiO_2 counterpart. Furthermore, the high degree of etch selectivity, created by combining the oxide with III-V materials, presents new opportunities to use the oxide as a sacrificial layer in micro-electro-mechanical structures and nano-electro-mechanical structures.[15,16] Recently, the use of low-index, oxidized Al-containing material has been employed in photonic bandgap crystal structures that require high dielectric contrast in their design.[7,17] In addition, broadband dielectric-stack structures that use oxidized low-index layers can be monolithically integrated with saturable absorbers for mode-locking ultrashort pulse lasers.[6,18]

By increasing the dimensions of oxidized Al layers to larger lateral dimensions and thicknesses, new technological applications become possible. For example, using large-area oxidized mirrors integrated with an absorber in a solid-state laser allowed for stable mode locking. The large area (500-μm-diameter circular mesa) lessened the effects of two photon absorption.[6,18] In addition, creating thick buried oxides can allow for sufficient index confinement over large areas in III-V planar lightwave circuits, creating new possibilities for device integration. To our knowledge, in the majority of the work that has been reported to date, the oxidation of Al-based materials has been limited to relatively small areas (tens of μm^2) or to relatively thin ($\lambda/4$) layers. Oxidation areas may have been limited due to the fact that the process of creating oxidized layers at larger dimensions can easily be degraded by the effects of structure delamination.

In this paper, various approaches are described to increase oxidation dimensions in both the horizontal and vertical directions, creating stable large-area and thick buried oxides. Fabrication process tradeoffs involve the oxidation times, the oxidation

(Received August 3, 2003; accepted January 30, 2004)

temperatures, and the composition of the Al-containing layers, each of which influences the stability and oxidation rate.

To illustrate both large-scale horizontal oxidation and large-scale vertical oxidation, two structure types are examined. The first structure is a 500-μm-diameter cylindrical dielectric stack composed of thin (hundreds of nanometers) alternating layers of high- and low-index material. The low-index layers are oxide layers created through the wet oxidation of Al-containing layers. The second structure is a semiconductor-on-insulator structure with a very thick, low-index oxide that is buried beneath a thinner GaAs device layer. Such a GaAs/oxide structure is analogous to widely used Si/SiO_2 silicon-on-insulator (SOI) structures.

EXPERIMENTAL

Two types of structures are discussed in this paper: large-area dielectric stacks with thin, multiple buried-oxide layers and large-area semiconductor-on-insulator structures with a thick buried-oxide layer. Both structure types were grown using gas-source molecular beam epitaxy (MBE) on GaAs (100) substrates. The growth temperature of the GaAs and $Al_xGa_{1-x}As$ layers was approximately 600°C. Because the MBE system contains only one Ga and Al cell, the growth rate of the AlGaAs layers is dependent on the desired Al content. For example, in the AlAs/$Al_{0.3}Ga_{0.7}As$ dielectric stack, the growth rates were 0.4 μm/h and 1.3 μm/h, respectively.

The Al-containing layers were oxidized in a tube furnace in which nitrogen gas carries water vapor from a heated bath to the sample located in a furnace tube. Syphons are used to maintain relatively constant water levels in the bath and bubbler during long oxidations. For all oxidations reported, the water bath temperature was maintained at an average temperature of 90°C. The furnace temperature was varied between 380°C and 475°C as measured by a thermocouple. The samples were prepared prior to oxidation either by cleaving the wafer to expose an edge facet, or by defining mesas using photolithography and wet etchants: a (1:1) $HCl:H_3PO_4$ solution to etch InP-based epilayers and a (1:8:40) $H_2SO_4:H_2O_2:H_2O$ solution to etch arsenic-containing layers.

The structures were characterized using a number of optical and structural analytical tools. High-resolution x-ray diffraction (400) rocking curves were used to determine the layer thicknesses of the unoxidized structures. After oxidation, plan view images were taken using a Nomarski microscope and cross-sectional images were taken using scanning electron microscopy (SEM). The Nomarski images highlighted the extent of the oxidation and any structural deformation. The SEM micrographs illustrated the oxidation front's progression through the layered structure and helped to identify any delaminated interfaces. Complete oxidation of the dielectric-stack structures was verified using reflectance measurements obtained with Fourier-transform infrared (FTIR) spectroscopy and a microspectrophotometer. Both measurement techniques measure the relative reflectance over a range of wavelengths using a reference metal mirror. Auger electron spectroscopy (AES) profile analyses were used to verify complete oxidation of the semiconductor-on-insulator structures.

RESULTS AND DISCUSSION

Dielectric Stacks

A number of dielectric-stack structures were studied with the goal of creating large-area heterostructures with alternating layers of high and low refractive-index material. In the simplest design, a structure with alternating layers of GaAs and AlAs was grown, and 500 μm circular mesas were fabricated and oxidized in an attempt to form $GaAs/Al_xO_y$ dielectric stacks. With its fast oxidation rate, AlAs was chosen as the oxidizing layer in order to achieve large areas of aluminum oxide. Upon oxidation, however, this type of structure can suffer from severe deformation. For example, Fig. 1a shows the deformation of one mesa after an oxidation at 435°C for 2 h. The cross section shown in Fig. 1b illustrates that the distortion is due to delamination between the GaAs (106-nm thick) and AlAs (240-nm thick) layers. Partial oxidation of the same dielectric-stack structure at 435°C for 45 min also showed severe delamination for both the oxidized and unoxidized regions of the structure. This illustrates that delamination effects caused by the oxidation process can propagate over the full area of the structure. Similar delamination has been observed in a number of cases and may be explained by the weak bonding between an interfacial GaAs oxide and Al_xO_y layers,[19,20] in addition to the stress created by AlAs volume contraction upon oxidation.[21] These stresses in the oxidized regions then allow the delamination process to propagate throughout the whole mesa structure as illustrated by Fig. 1a and b. Lowering the oxidation temperature lessens the delamination effects but with the tradeoff of increased oxidation times. Figure 2a shows that by lowering the oxidation temperature to 375°C, a 10-h oxidation only partially oxidized the mesa (140 μm from the edge) but eliminated the delamination effects. At temperatures above 375°C, faster oxidation rates are achieved but with increasing delamination effects.

Instead of varying the oxidation temperature to stabilize the structures, variations in material composition were considered as an alternative. To strengthen the bonding between the high-index layers and the oxide layers, aluminum was added to the high-index GaAs layer of the dielectric-stack structure. Because AlGaAs has a substantially lower oxidation rate than AlAs,[19] an $Al_{0.7}Ga_{0.3}As$ layer was initially considered for the high-index layer. Figure 2b shows a 500-μm-diameter mesa with an $Al_{0.7}Ga_{0.3}As$ (130 nm)/AlAs (240 nm) stacked structure that was completely oxidized in 2 h at 435°C with no deformation of the layered structure. (The slight edge delami-

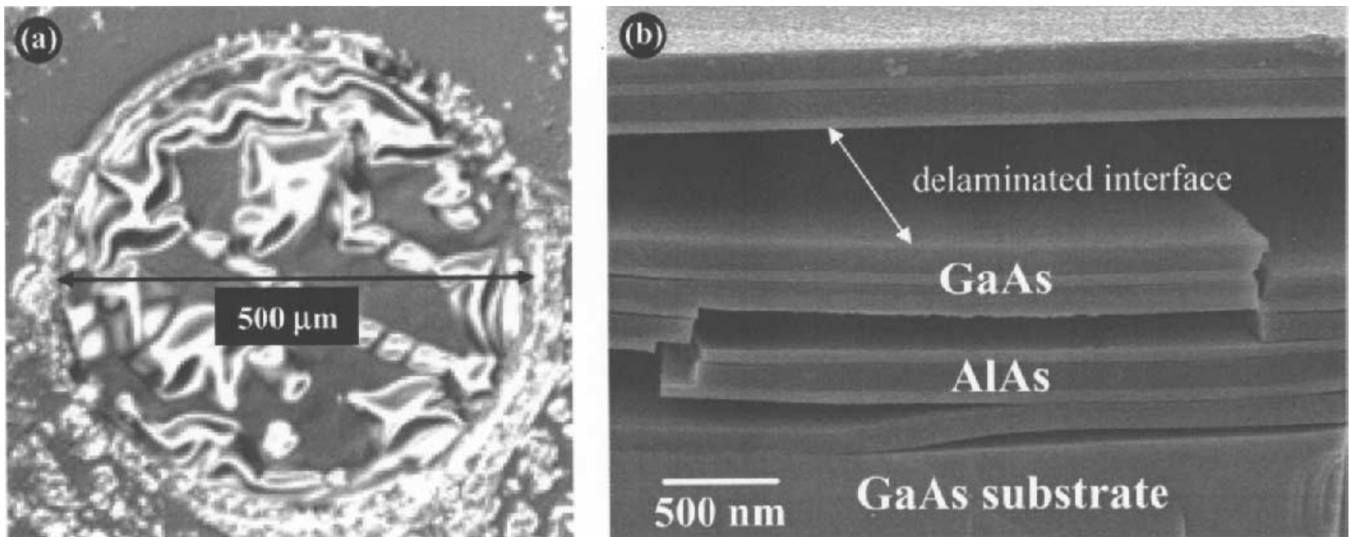

Fig. 1. (a) Nomarski micrograph showing the plan view of a GaAs/AlAs dielectric stack deformed because of stresses introduced by oxidation at 435°C for 2 h. (b) An SEM image showing the cross section of the stack with delaminated layers.

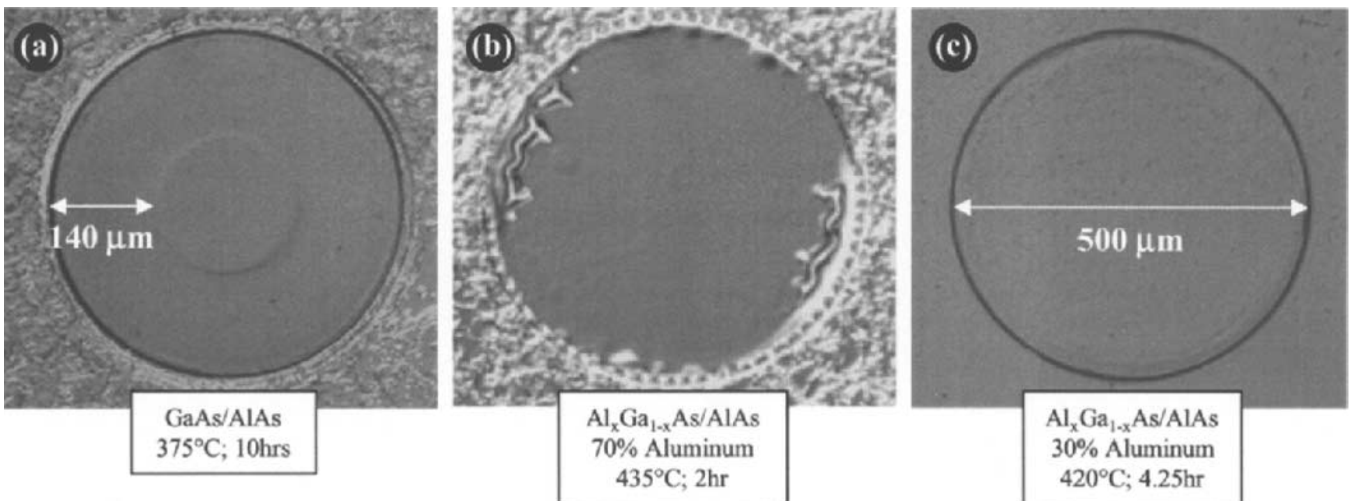

Fig. 2. Nomarski micrographs showing the plan views of three different seven-pair dielectric-stack structures after oxidation: (a) a GaAs/AlAs structure oxidized at 375°C for 10 h, (b) an $Al_{0.7}Ga_{0.3}As$/AlAs structure oxidized at 435°C for 2 h, and (c) an $Al_{0.3}Ga_{0.7}As$/AlAs structure oxidized at 420°C for 4.25 h.

nation that is observed is at the interface between the uppermost oxide layer and a highly strained, InP top layer.) The SEM images suggested, however, that although the dielectric-stack structure successfully endured the stresses of oxidation, oxidation of the $Al_{0.7}Ga_{0.3}As$ layers was significant—especially toward the edges of the mesa where complete oxidation of all the AlAs and AlGaAs layers had occurred.

To slow the oxidation rate of the $Al_xGa_{1-x}As$ layer so as to retain its high refractive index after oxidation, the aluminum content was decreased to 30%. Figure 2c shows that an oxidation at 420°C for 4.25 h resulted in the complete oxidation of the mesa with no delamination of the $Al_{0.3}Ga_{0.7}As$ (92 nm)/AlAs (200 nm) layered structure. The SEM images also suggested no significant oxidation of the AlGaAs layer.

Reflectivity measurements taken using FTIR spectroscopy and a microspectrophotometer were used to characterize the performance of the dielectric stack as a mirror. The reflectance measurements, shown in Fig. 3, contrast the reflectivities of the oxidized and unoxidized $Al_{0.3}Ga_{0.7}As$ (92 nm)/AlAs (200 nm) structures. The high dielectric contrast between layers in the oxidized structure creates a mirror with high reflectivity over a broad wavelength range. This measurement verifies that after the oxidation process, high dielectric contrast stacks were created without noticeable oxidation of the high-index layers. Therefore, low Al-content AlGaAs layers can be used as the high-index layer of a dielectric stack to help stabilize the structure during large-area oxidations.

Thick Oxides

The large-scale oxidation of AlAs layers was also considered for the creation of thick buried-oxide layers for semiconductor-on-insulator structures. As an initial experiment, an oxidation was performed on a GaAs-based structure consisting of a 450-nm-thick GaAs layer on a 3,000-nm-thick AlAs layer. Two

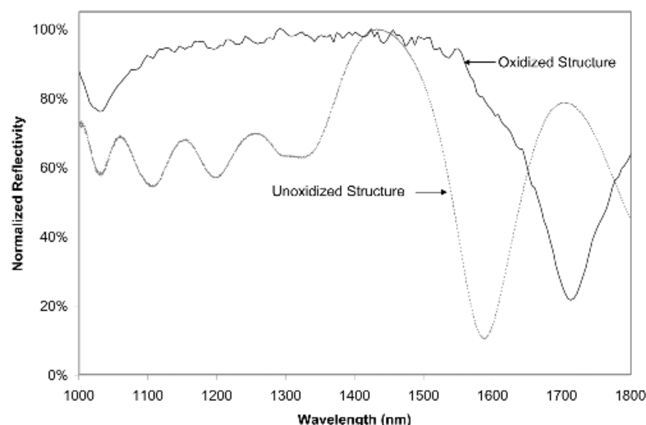

Fig. 3. Reflectance measurements of the oxidized and unoxidized $Al_{0.3}Ga_{0.7}As$/AlAs dielectric-stack structures.

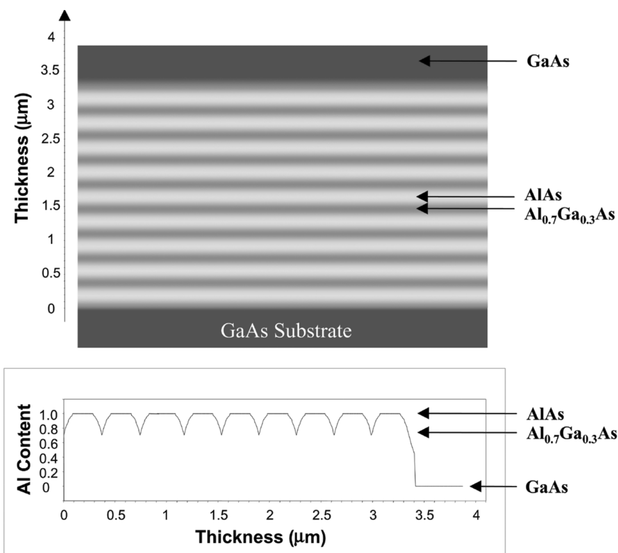

Fig. 4. Schematic illustrating the cross section of the structure used to create a thick buried oxide with a plot of the designed aluminum content as a function of structure thickness.

50-nm $Al_{0.50}Ga_{0.50}As$ layers were grown at both interfaces of the AlAs layer. The goal was to completely oxidize the 3,000-nm-thick AlAs layer, creating a thick buried oxide using 50-nm intermediary $Al_{0.50}Ga_{0.50}As$ layers to reduce the strain between the oxide and the GaAs epilayer and underlying substrate. Three oxidation runs were performed on cleaved samples of the above structure at temperatures of 470°C, 430°C, and 400°C for 1 h. All three runs resulted in severe deformation of the structure. This deformation was likely caused by the lattice contraction of the very thick AlAs layer, which strained the AlGaAs intermediary layers and the GaAs top layer. With a 3,000-nm AlAs layer, a 12% linear contraction[21] would result in a 360-nm contraction approaching the layer thickness of the 450-nm GaAs top layer.

This experiment illustrates that even by lowering the oxidation temperature, oxidizing a thick buried layer of AlAs will not result in a stable structure. Varying the aluminum composition of the heterostructure was again considered as an alternative. Oxidations performed on the dielectric stacks illustrated that GaAs/AlAs structures are not suitable for large-scale oxidations and that the use of AlGaAs instead of GaAs stabilized these structures. Low Al-content AlGaAs stabilized the structure without significant oxidation, whereas high Al-content AlGaAs stabilized the structure with significant oxidation.

Using these results, the semiconductor-on-insulator structure was modified to reduce the volume contraction of the oxidizing layer while allowing for reasonable oxidation times. The approach uses alternating layers of AlAs and high Al-content AlGaAs to create a thick aluminum layer that can be completely oxidized as in the dielectric-stack case that was presented in Fig. 2b. By using the layered structure, the high oxidation rates of AlAs layers can be combined with the lower volume contraction of AlGaAs layers[21] to create thick buried oxides over a large area. A schematic of the structure is shown in Fig. 4. To stabilize the structure even further, the interfaces between each AlAs and AlGaAs layer were continuously graded during the MBE growth to reduce interfacial stresses upon oxidation.

Figure 5a–d illustrates the oxidation results of a cleaved sample from the structure illustrated in Fig. 4 after steam oxidation at 420°C for 11 h. A sequence of SEM images, obtained along the path of the oxidation front, shows how the thick layered structure becomes fully oxidized. After 11 h, the oxidation front advanced ~500 µm from the sample edge. Figure 5a shows a cross-sectional profile at the oxide terminus. The oxide terminus of two of the oxidized AlAs layers is clearly shown because of the contrast between AlAs and Al_xO_y. The AlGaAs layers, between the oxidized AlAs layers, remain unoxidized. Figure 5b shows a cross-sectional image further away from the oxide terminus, approximately 400 µm from the sample edge. Three oxidized AlAs layers are shown between the AlGaAs layers that are now partially oxidized in the vertical direction. The oxidized AlGaAs appears brighter and with more contrast than the oxidized AlAs. Figure 5c, which is an image approximately 300 µm from the sample edge, shows how the vertical oxidation of the AlGaAs layers has progressed even further, leaving only thin, unoxidized AlGaAs layers surrounded by thicker oxide layers. In Fig. 5d, the cross-sectional image at an area closest to the sample edge shows a completely oxidized structure.

Though the lateral oxidation rate of AlGaAs is slow, the AlAs layers, which oxidize more quickly, allow for subsequent vertical oxidation of the adjacent AlGaAs layers. Thus, the effective rate of oxidation of the AlGaAs layers is increased. In addition, because the AlAs layers experience a greater contraction than the AlGaAs layers, the overall lattice contraction in this structure has decreased relative to the pure AlAs case, resulting in a stable, thick buried-oxide layer.

The AES analysis verified complete oxidation of the structure, as shown in Fig. 6. Because Auger-electron energies carry a unique signature of the element from which they were emitted, compositional

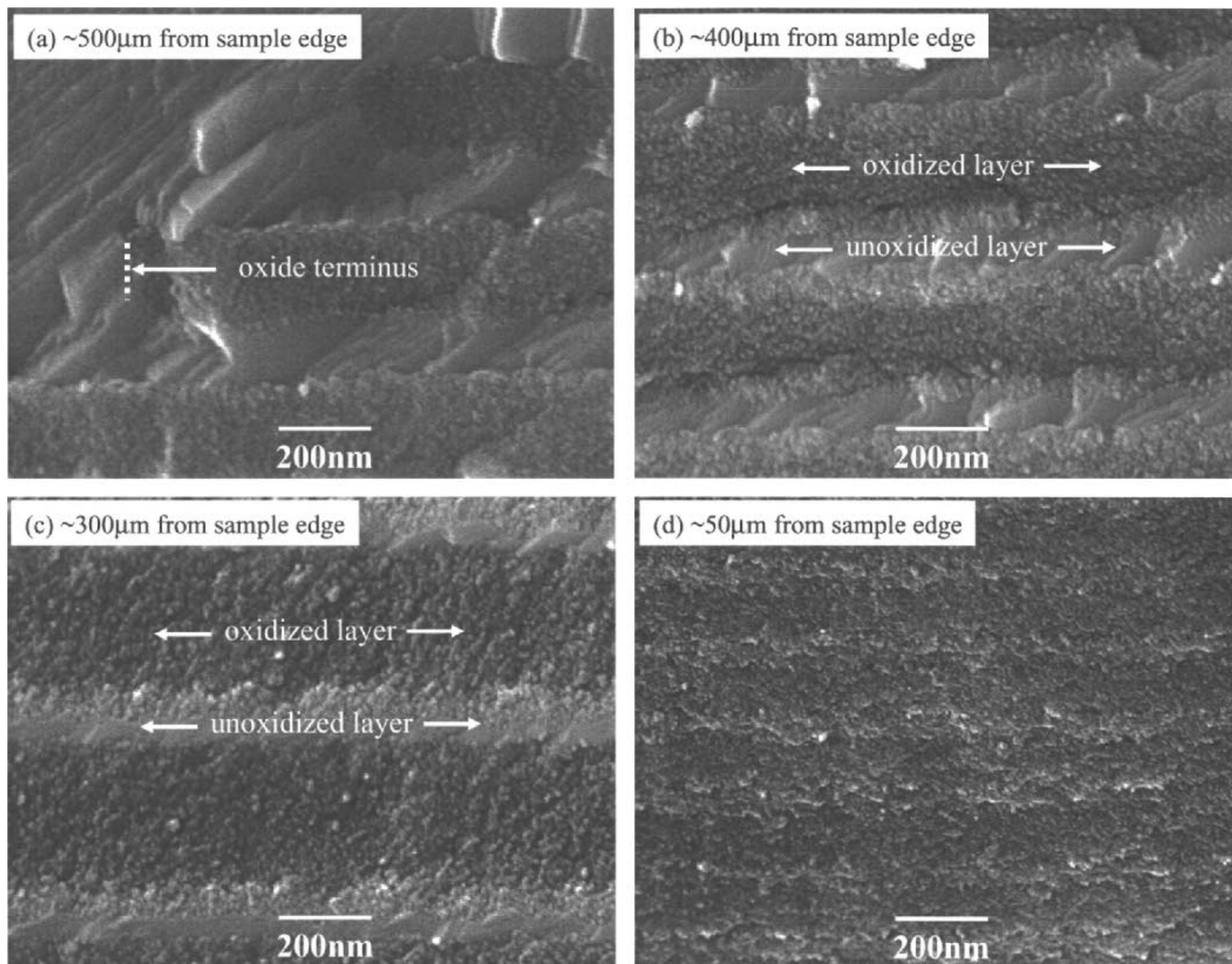

Fig. 5. The SEM micrographs at different locations from the sample edge show lateral oxidation of AlAs layers with subsequent vertical oxidation of the AlGaAs layers. (Schematic of the structure is shown in Fig. 4.)

analysis was performed to detect the presence of aluminum, arsenic, gallium, and oxygen at different depths in the layered structure. Cycles of ion sputtering followed by analysis steps with a 3-keV electron beam were used to obtain compositional information versus depth. In Fig. 6, the relative elemental concentrations after each sputtering cycle are demonstrated using a plot of the Auger-electron intensity versus energy. The native gallium oxide is detected through the presence of oxygen and gallium Auger-electron intensities in the first two analysis cycles. The top GaAs layer is identified through the gallium and arsenic Auger-electron intensities of cycles 3 through 19. After analysis cycle 19, the arsenic Auger-electron intensity rapidly decreases, and the aluminum and oxygen intensities increase. The grading of the gallium content in the oxidized AlGaAs layer is also visible at cycles 19 and 54 through the slight increase in the gallium Auger-electron intensities. The oxygen content remains approximately flat until completion of the AES scan in cycle 60 verifying the complete oxidation of the top AlAs/AlGaAs layers in the structure.

This experiment shows that thick, buried Al_xO_y layers can be created without delamination by oxidizing a stacked AlAs/AlGaAs structure. In addition, this oxidation shows that such layers can be created over millimeter-scale areas. The preceding oxidation at 420°C for 11 h was performed for a sample with a cleaved facet and resulted in an oxidation rate of about 0.8 μm/min for the AlAs layers. Oxidations performed on large-area square-shaped mesas defined with photolithography and wet etchants resulted in similar oxidation rates. Faster oxidation rates were observed for circular-shaped mesas. For example, the oxidation front progressed approximately 160 μm from the edge of a 500-μm circular mesa after a 2-h oxidation at 420°C. This implies an oxidation rate of 1.3 μm/min. Therefore, temperature, time, and geometry must be considered to maximize the oxidation rates to create millimeter-scale oxide areas. However, long oxidation times at higher temperatures can also result in the oxidation of GaAs layers. The SEM images and an AES scan verified significant oxidation of the top GaAs surface after only 1 h of oxidation at 470°C. Lower temperatures slow this oxidation rate

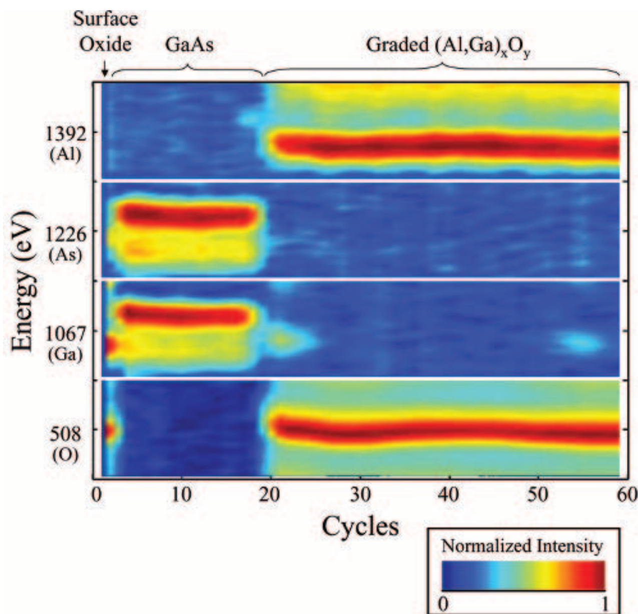

Fig. 6. The AES profile verifying complete oxidation of the layered structure. The presence of each element is detected through the peaks in detected intensity at the characteristic Auger-electron energies.

significantly. A cap layer of SiO_2 has been shown to protect the GaAs layer during oxidation.

SUMMARY

By engineering the aluminum content of heterostructures, the wet oxidation of Al-based structures can be successfully accomplished at large dimensions in the vertical and horizontal directions. This was demonstrated using two types of structures: large-area dielectric-stack structures with multiple layers of thin buried oxides and semiconductor-on-insulator structures with a thick buried oxide. Creating a large-area oxide structure requires the design of a heterostructure that can oxidize quickly while remaining stable during the oxidation process. AlAs is used as the main oxidizing layer for both structure types because it has the fastest oxidation rate. In the dielectric-stack structures, using GaAs as the high-index layer leads to delamination at the oxide interfaces because of weak bonding. As an alternative, low Al-content AlGaAs layers with very low oxidation rates are used as substitutes for GaAs layers. The result is an increase in the stability of the structure after oxidation, allowing for the creation of large-area dielectric stacks. In semiconductor-on-insulator structures with a thick buried oxide, using thick AlAs as the oxidizing layer leads to deformation of the structure caused by volume contraction. Alternatively, high Al-content AlGaAs layers are inserted between AlAs layers to lower the overall volume contraction of the structure with oxidation occurring in the vertical and horizontal directions. The result is the creation of stable structures that can be successfully oxidized over millimeter-scale areas.

ACKNOWLEDGEMENTS

The authors thank Dr. Jumi Lee, CRAIC Technologies, for the reflectivity measurement of the oxidized dielectric-stack structure using the QDI 1000 NIR microspectrophotometer. In addition, many thanks to Professor Franz Kaertner and Dr. Thomas Schibli for their collaboration on the use of large-area dielectric-stack structures in ultrashort pulse lasers. The work described here was funded by Rockwell Science Company LLC (Thousand Oaks, CA) through the Office of Naval Research (ONR) Contract No. N66001-00-C-8068 and by ONR Award No. N00014-02-1-0717. This work also made use of the Shared Experimental Facilities supported in part by the MRSEC Program of the National Science Foundation under Award No. DMR 02-13282.

REFERENCES

1. J.M. Dallesasse and N.J. Holonyak, *Appl. Phys. Lett.* 58, 394 (1991).
2. F.A. Kish, S.J. Caracci, N.J. Holonyak, J.M. Dallesasse, K.C. Hsieh, M.J. Ries, S.C. Smith, and R.D. Burnham, *Appl. Phys. Lett.* 59, 1755 (1991).
3. S.A. Maranowski, A.R. Sugg, E.I. Chen, and N. Holonyak, Jr., *Appl. Phys. Lett.* 63, 1660 (1993).
4. K.D. Choquette, R.P. Schneider, K.L. Lear, and K.M. Geib, *Electron. Lett.* 30, 2043 (1994).
5. G.M. Yang, M.H. MacDougal, and P.D. Dapkus, *Electron. Lett.* 31, 886 (1995).
6. D.J. Ripin, J.T. Gopinath, H.M. Shen, A.A. Erchak, G.S. Petrich, L.A. Kolodziejski, F.X. Kaertner, and E.P. Ippen, *Opt. Comm.* 214, 285 (2002).
7. A.A. Erchak, D.J. Ripin, S. Fan, P. Rakich, J.D. Joannopoulos, E.P. Ippen, G.S. Petrich, and L.A. Kolodziejski. *Appl. Phys. Lett.* 78, 563 (2001).
8. M.H. MacDougal, H. Zhao, P.D. Dapkus, M. Ziari, and W.H. Steier, *Electron. Lett.* 30, 1147 (1994).
9. M.H. MacDougal, P.D. Dapkus, V. Pudikov, and H.G.M. Yang, *IEEE Photonic. Technol.* 7, 229 (1995).
10. S.J. Caracci, M.R. Krames, N. Holonyak, Jr., C.M. Herzinger, A.C. Crook, T.A. DeTemple, and P.A. Besse, *Appl. Phys. Lett.* 63, 2265 (1993).
11. D.J. Ripin, K. Lim, G.S. Petrich, P.R. Villeneuve, S. Fan, E.R. Thoen, J.D. Joannopoulos, E.P. Ippen, and L.A. Kolodziejski, *J. Lightwave Technol.* 17, 2152 (1999).
12. W.T. Tsang, M. Olmstead, and R.P.H. Chang, *Appl. Phys. Lett.* 34, 408 (1979).
13. E.I. Chen, N. Holonyak, Jr., and S.A. Maranowski, *Appl. Phys. Lett.* 66, 2688 (1995).
14. P.A. Grudowski, R.V. Chelakara, and R.D. Dupuis, *Appl. Phys. Lett.* 69, 388 (1996).
15. K. Lim, D.J. Ripin, G.S. Petrich, P.R. Villeneuve, S. Fan, J.D. Joannopoulos, E.P. Ippen, and L.A. Kolodziejski, *Adv. Mater.* 11, 501 (1999).
16. M.L. Povinelli et al., *IEEE Photonic. Technol. Lett.* 15, 1207 (2003).
17. E. Chow, S.Y. Lin, J.R. Wendt, S.G. Johnson, and J.D. Joannopoulos, *Opt. Lett.* 26, 286 (2001).
18. T.R. Schibli, J. Kim, O. Kuzucu, J.T. Gopinath, S.N. Tandon, G.S. Petrich, L.A. Kolodziejski, E.P. Ippen, and F.X. Kaertner, *Opt. Lett.* 28, 947 (2003).
19. K. Choquette, K. Geib, H. Chui, B. Hammons, H. Hou, T. Drummond, and R. Hull. *Appl. Phys. Lett.* 69, 1385 (1996).
20. P. Evans, J. Wierer, and N. Holonyak, Jr. *J. Appl. Phys.* 84, 5436 (1998).
21. M. MacDougal and P. Dapkus, *IEEE Photonic. Technol. Lett.* 9, 884 (1997).